Supporting Information for

Positional Effects of Fluorination in Conjugated Side Chains on Photovoltaic Properties of Donor-Acceptor Copolymers

Jisoo Shin‡, Min Kim‡, Jaewon Lee, Heung Gyu Kim, Hyeongjin Hwang, and Kilwon Cho*

Department of Chemical Engineering
Pohang University of Science and Technology
Pohang 790-784, Korea

Email : kwcho@postech.ac.kr

Table of contents

Experimental

Materials

All materials including chemicals and solvents from commercial sources were used without further purifications. 5,6-difluoro-4,7-bis(5-bromo-4-(2-ethylhexyl)-2-thienyl)-2,1,3-benzothiadiazole (M3) was synthesized according to reported methods.[1] All monomers were synthesized as shown in Scheme S1. To probe the positional effect of fluorination in phenyl side chain attached to polymer backbone, two corresponding polymers (PPh-*m*-F and PPh-*o*-F) with alkoxyphenyl-substituted benzo[1,2-b:3,4-b′]dithiophenes (BDTs) were synthesized as shown in Scheme S2. Synthetic route and result of PPh is referred to Ref. 2.

Synthesis of Monomers

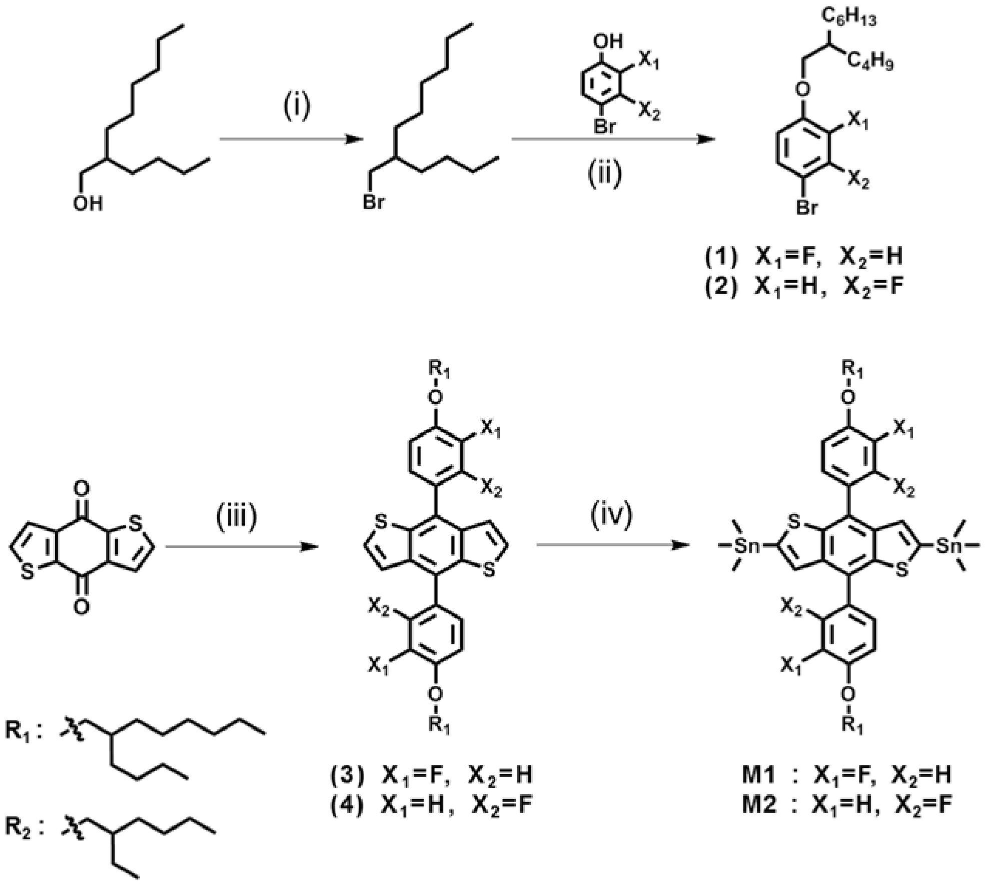

Scheme S1. Synthetic procedures of electron donating monomers; BDT-Ph-*m*-F and BDT-Ph-*o*-F. i) PPh$_3$, Br$_2$, r.t., 12h, ii) K$_2$CO$_3$, r.t., 48 h, iii) n-butyl lithium, SnCl$_2$, THF, 55 ºC, overnight, iv) n-butyl lithium, trimethyltin chloride, THF, -75 ºC, overnight.

1-Bromo-4-(2’-butyloctyloxy)-3-fluorobenzene (1). Under nitrogen atmosphere, 4-bromo-2-fluorophenol (8.0 g, 42 mmol), K_2CO_3 (6.4 g, 46 mmol) were put into three-neck round bottom flask with 100 ml DMSO. 1-Bromo-butyloctane (2) (11.5 g, 46 mmol) was added dropwise in room temperature. The mixture was stirred 48 h and the mixture was poured into 200 ml ice cold water and then extracted with ethylacetate three times. Organic layer was washed with water and dried over magnesium sulfate and evaporated to get crude product. The crude product was purified on a silica gel column with hexane. Clear oil is obtained (12.7 g, 84 %). ^{1}H NMR ($CDCl_3$, 400 MHz), δ (ppm): 7.22 (d, 1H), 7.16 (d, 1H), 6.82 (t, 1H), 3.86 (d, 2H), 1.80 (m, 1H), 1.48-1.27 (m, 16H), 0.91-0.87 (m, 6H). ^{13}C NMR (400 MHz, $CDCl_3$), δ (ppm): 153.54, 151.88, 146.95, 146.88, 127.11, 127.08, 119.70, 119.56, 116.07, 116.06, 111.70, 111.64. 72.64, 37.91, 31.83, 31.21, 30.89, 29.64, 29.00, 26.76, 23.02, 22.67, 14.10, 14.07

4,8-Bis(4-butyloctyloxy-3-fluroro-1-phenyl)-benzo[1,2-b:4,5-b’]-dithiophene (3). Under nitrogen atmosphere, 1-bromo-4-(2’-butyloctyloxy)-3-fluorobenzene (3) (8.0 g, 22 mmol) was dissolved in dry THF (40 ml) and then n-butyllithium solution (22 mmol, 8.9 mL, 2.5 M in n-hexane) was added dropwise at -78 °C. After addition, the reaction mixture was maintained at -78 °C for 2 h, followed by the addition of benzo[1,2-b:4,5-b′]dithiophene-4,8-dione (4) (1.37 g, 7.4 mmol) and allowed to warm to 55 °C for 2 h. The solution was cooled down and then $SnCl_2 \cdot 2H_2O$ (13.6 g, 60 mmol) in 10 % aqueous HCl (30 mL) was added. The solution was refluxed for 6 h and then the cooled the mixture was poured into water and extracted with dichloromethane, the organic extraction was washed successively with water and sodium bicarbonate solution twice and the combined organic phase was dried over magnesium sulfate and evaporated to afford the crude product. The crude product was purified on a silica gel column, eluting with pure hexane. White crystals were obtained (2.76 g, 50 % yield). ^{1}H NMR ($CDCl_3$, 400 MHz), δ (ppm): 7.47 (m, 6H), 7.38 (d, 2H), 7.16 (t, 2H), 4.08 (d, 4H), 1.94 (m, 2H), 1.58-1.28 (br, 32H), 0.93 (m, 12H). ^{13}C NMR (400 MHz, $CDCl_3$), δ (ppm): 153.75, 152.11, 147.54, 147.46, 138.32, 136.21, 132.04, 131.99, 129.24, 127.34, 125.26, 125.24, 122.75, 117.38, 117.26, 115.39, 77.15, 76.93, 76.72, 72.85, 38.20, 31.81, 31.45, 31.12, 29.64, 29.11, 26.85, 23.00, 22.61, 13.96, 13.93

2,6-Bis(trimethyltin)-4,8-Bis(4-butyloctyloxy-3-fluoro-1-phenyl)-benzo[1,2-b:4,5-b’]-dithiophene (M1). A solution of compound (6) (0.64 g, 0.8 mmol) in dry THF (10 ml) was stirred under nitrogen gas for 30 min, and then 2.5 M n-butyllithium solution in hexane (1 ml) was added dropwise at -78 °C. Then the solution was kept at -78 °C for 1 h, and 1.0 M trimethyltin chloride solution in THF (2.5 ml) was added. Then the solution was allowed to warm up to room temperature and stirred overnight. The mixture was poured into water and extracted with ether. The organic phase was evaporated, and the crude product was purified by recrystallization in ethanol to afford pale yellow needles (0.73 g, yield 85 %). ^{1}H NMR ($CDCl_3$, 400 MHz), δ (ppm): 7.46 (d, 4H), 7.38 (s, 2H), 7.18 (t, 2H), 4.06 (d, 4H), 1.94 (m, 2H), 1.57-1.35 (br, 32H), 0.93 (m, 12H), 0.39 (t, 18H). ^{13}C NMR ($CDCl_3$, 100 MHz), δ (ppm): 153.47, 151.84, 147.25, 147.19, 142.53, 142.35, 136.97, 132.46, 130.45, 127.57, 125.32, 125.30, 117.39, 117.27, 114.80, 77.01, 76.80, 72.35, 38.08, 31.88, 31.36, 31.05, 29.71, 29.10, 26.86, 23.08, 22.70, 14.13, 14.12. Elemental analysis: calcd : $C_{52}H_{76}$ $F_2O_2S_2Sn_2$: C, 58.22 ; H, 7.14 ; S, 5.98 found : C, 58.87 ; H, 6.69 ; S, 5.83. MALDI TOF MS: m/z 1072.19

1-Bromo-4-(2’-butyloctyloxy)-2-fluorobenzene (2). A stirred mixture of 4-bromo-3-fluorophenol (7.0 g, 37 mmol), K_2CO_3 (5.6 g, 40 mmol) were put into three-neck round bottom flask with 100 ml DMSO. 1-Bromo-butyloctane (2) (10.0 g, 40 mmol) was added dropwise in room temperature. The mixture was stirred 48 h and the mixture was poured into 200 ml ice cold water and then extracted with ethylacetate three times. Organic layer was washed with water and dried over magnesium sulfate and evaporated to get crude product. The crude product was purified on a silica gel column with hexane. Clear oil is obtained (11.3 g, 85 %). ^{1}H NMR ($CDCl_3$, 400 MHz), δ (ppm): 7.41 (d, 1H), 6.71 (d, 1H), 6.63 (t, 1H), 3.81 (d, 2H), 1.80 (m, 1H), 1.48-1.27 (m, 16H), 0.91-0.87 (m, 6H).

4,8-Bis(4-butyloctyloxy-2-fluroro-1-phenyl)-benzo[1,2-b:4,5-b’]-dithiophene (4). Under nitrogen atmosphere, 1-bromo-4-(2’-butyloctyloxy)-2-fluorobenzene (4) (10.0 g, 28 mmol) was dissolved in dry THF (40 mL) and then n-butyllithium solution (28 mmol, 11.1 mL, 2.5 M in n-hexane) was added dropwise at -78 °C. After addition, the reaction mixture was maintained at -78 °C for 2 h, followed by the addition of benzo[1,2-b:4,5-b′]dithiophene-4,8-dione (4) (1.71 g, 9.3 mmol) and allowed to warm to 55 °C for 2 h. The solution was cooled down and then $SnCl_2\cdot{}_2H_2O$ (17.0 g, 75 mmol) in 10 % aqueous HCl (22 mL) was added. The solution was refluxed for 6 h and then the cooled the mixture was poured into water and extracted with dichloromethane, the organic extraction was washed successively with water and sodium bicarbonate solution twice and the combined organic phase was dried over magnesium sulfate and evaporated to afford the crude product. The crude product was purified on a silica gel column, eluting with pure hexane. White crystals were obtained (3.5 g, 50 % yield). ^{1}H NMR ($CDCl_3$, 400 MHz), δ (ppm): 7.57 (d, 2H), 7.42 (m, 2H), 7.20 (t, 2H), 6.92 (m, 4H), 3.97 (d, 4H), 1.89 (m, 2H), 1.62–1.33 (br, 32H), 0.91 (m, 12H). ^{13}C NMR ($CDCl_3$, 100 MHz), δ (ppm): 161.21, 159.59, 142.97, 141.86, 137.62, 132.10, 131.94, 130.73, 122.84, 118.71, 110.80, 102.50, 78.80, 71.34, 38.00, 31.88, 31.43, 29.71, 26.89, 23.09, 22.70, 14.13

2,6-Bis(trimethyltin)-4,8-Bis(4-butyloctyloxy-2-fluoro-1-phenyl)-benzo[1,2-b:4,5-b’]-dithiophene (M2). A solution of compound (8) (0.7 g, 0.9 mmol) in dry THF (15 ml) was stirred under nitrogen gas for 30 min, and then 2.5 M n-butyllithium solution in hexane (1.2 ml) was added dropwise at -78 °C. Then the solution was kept at -78 °C for 1 h, and 1.0 M trimethyltin chloride solution in THF (3 ml) was added. Then the solution was allowed to warm up to room temperature and stirred overnight. The mixture was poured into water and extracted with ether. The organic phase was evaporated, and the crude product was purified by recrystallization in ethanol to afford pale yellow needles (0.75 g, yield 78 %). ^{1}H NMR ($CDCl_3$, 400 MHz), δ (ppm): 7.55 (d, 2H), 7.21 (s, 2H), 6.92 (d, 2H), 6.88 (d, 2H), 3.97 (d, 4H), 1.85 (m, 2H), 1.57-1.34 (br, 32H), 0.95 (m, 12H), 0.38 (t, 18H). ^{13}C NMR ($CDCl_3$, 100 MHz), δ (ppm): 162.19, 161.84, 161.76, 143.95, 142.83, 139.62, 139.17, 138.60, 137.20, 132.96, 132.93, 131.71, 128.01, 123.85, 119.81, 111.78, 103.66, 103.49, 78.20, 77.99, 77.78, 72.32, 38.98, 32.86, 32.10, 30.69, 30.12, 30.10, 27.88, 27.86, 24.07, 23.69, 15.11. Elemental analysis: calcd : $C_{52}H_{76}$ $F_2O_2S_2Sn_2$: C, 58.22 ; H, 7.14 ; S, 5.98 found : C, 58.87 ; H, 6.69 ; S, 5.83. MALDI TOF MS: m/z 1072.20

Synthesis of Polymers

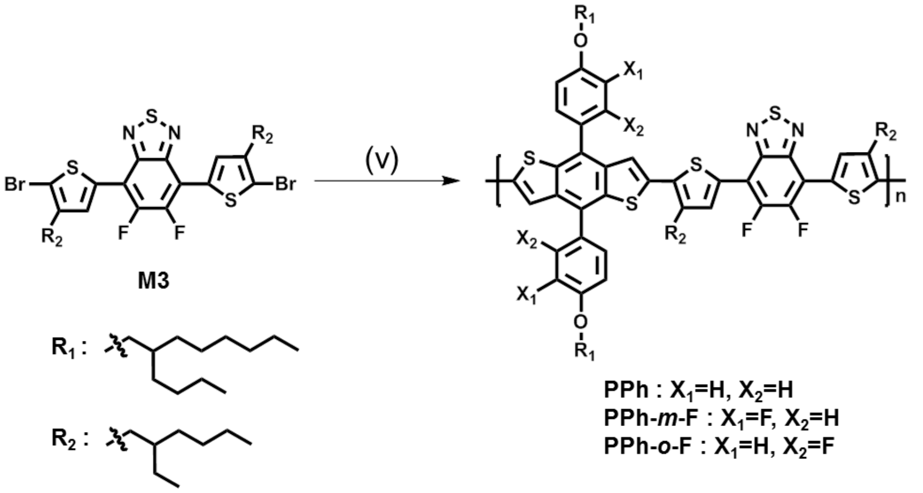

Scheme S2. Synthetic procedures of polymers; PPh (Ref.2), PPh-*m*-F, PPh-*o*-F. v) Polymerization condition: M1 or M2, $Pd(PPh_3)_4$, toluene/DMF (9:1), 110 °C reflux, 48 h.

PPh-*m*-F. M2 (321.8 mg, 0.3 mmol) and M5 (215.6 mg, 0.3 mmol) in 9 mL of anhydrous toluene and 1mL of DMF were put into a two-necked flask. The solution was refluxed at 110 °C for 48 h under nitrogen, followed by end-capping using 2-tributyltinthiophene and 2-bromothiophene, successively. After cooling down to room temperature, the solution was quenched in methanol, filtered, and then purified by Soxhlet extraction successively with methanol, acetone, hexane, chloroform and CB. Finally, the CB fraction was concentrated, and then the concentrate was precipitated in methanol. The dark blue solid was obtained after filtering and dried overnight in 62 % yield. ^{1}H NMR (500 MHz, *o*-dichlorobenzene-d_5): δ 8.29-8.19 (br, 2H), 7.63-7.51 (br, 6H), 6.90-6.88 (br, 2H), 4.12-4.01 (br, 4H), 3.02-2.80 (br, 4H), 1.88-1.31 (br, 48H), 0.90-0.82 (br, 24H), GPC (o-DCB, 80 °C): M_n = 12.3 kDa, PDI= 2.33

PPh-*o*-F. M4 (321.8 mg, 0.3 mmol) and M5 (215.6 mg, 0.3 mmol) in 9 mL of anhydrous toluene and 1mL of DMF were put into a two-necked flask. The solution was refluxed at 110 °C for 48 h under nitrogen, followed by end-capping using 2-tributyltinthiophene and 2-bromothiophene, successively. After cooling down to room temperature, the solution was quenched in methanol, filtered, and then purified by Soxhlet extraction successively with methanol, acetone, hexane, and chloroform. Finally, the chloroform fraction was concentrated, and then the concentrate was precipitated in methanol. The dark purple solid was obtained after filtering and dried overnight in 71 % yield. ^{1}H NMR (500 MHz, *o*-dichlorobenzene-d_5): δ 8.20-8.09 (br, 2H), 7.62-7.17 (br, 6H), 6.90-6.88 (br, 2H), 4.04-4.00 (br, 4H), 2.02-1.85 (br, 4H), 1.54-1.19 (br, 48H), 0.82-0.88 (br, 24H), GPC (o-DCB, 80 °C): M_n = 15.8 kDa, PDI= 1.50

Analysis

The molecular weights of the polymers were determined using high temperature gel permeation chromatography (GPC) with ***o***-DCB as eluent and polystyrene as the standard at 90 °C. The number and weight average molecular weights (M_n and M_w), polydispersity index (PDI), and decomposition temperature (T_d) of PPh-*m*-F and PPh-*o*-F were measured in Table 1. The thermal stability of these two polymers was investigated using thermo-gravimetric analysis (TGA) (Fig. S1). Both polymers exhibited good thermal stabilities, with onset decomposition temperatures (5 % weight loss) at 422 °C and 424 °C in an inert atmosphere. Neither clear transitions nor endothermic or exothermic behaviors were observed between 30 °C and 250 °C in differential scanning calorimetry (DSC) experiments**.**

Electrochemistry Electrochemical cyclic voltammetry (CV) was conducted on a PowerLab/AD instrument model system (glassy carbon disk as working electrode, Pt wire as counter electrode, Ag/AgCl as reference electrode) in a 0.1 M tetrabutyl ammonium hexafluorophosphate (n-Bu_4NPF_6)-anhydrous acetonitrile solution at a potential scan rate of 50 mV s^{-1} . Polymer films were drop cast onto the glassy carbon working electrodes from a 2.0 mg mL^{-1} hot CB solution and dried under nitrogen prior to measurements. The electrochemical onsets were determined at the position at which the current starts to differ from the baseline. The potential of the Ag/AgCl reference electrode was internally calibrated using the ferrocene/ferrocenium redox couple (Fc/Fc+). The energy levels were estimated: HOMO = – (4.80 + $E_{\text{onset, ox}}$), and LUMO = – (4.80 + $E_{\text{onset, red}}$).

Computational Studies. Density functional theory (DFT) calculations were performed using Gaussian 09 software package to obtain an in-depth understanding of the electronic structure of the designed polymers. Hybrid three-parameter B3LYP functional combined with the 6-31G (d) basis set was used to obtain the optimized structures at the singlet ground state. For simplicity, the 2-butyloctyl- and 2-ethylhexyl alkyl chains appended to the conjugated backbone and side aromatic chains were trimmed with methyl chains at the branch positions. HOMO and LUMO energy levels were analyzed using minimized singlet geometries to approximate the ground state.

Grazing Incidence Wide Angle X-ray Scattering (GIWAXS) analysis. Grazing incidence X-ray Wide Angle X-ray Scattering (GIWAXS) measurements were performed using Beamline 3C, 9A at the Pohang Accelerator Laboratory (PAL). The two dimensional GIXS images from the films were analyzed according to the relationship $q = 2\pi/d$ between the scattering vector q and the d spacing. The GIWAXS images shown are normalized with respect to exposure time.

Fabrication and Characterization of Organic Solar Cell Devices

ITO glasses were used as the anodes and cleaned by sequential sonication using detergent aqueous solution, deionized water, isopropyl alcohol, and acetone. After UV/ozone treatment for 30 minute, for photovoltaic devices with a MoO_3 interlayer, a MoO_3 film (9 nm) was thermally evaporated with a rate of 0.1 nm s^{-1} on UV-treated ITO substrates. Polymers and $PC_{71}BM$ were dissolved in *o*-DCB and the blend solutions were kept at a high temperature (90 °C) for more than one day. All processes were carried out in a glovebox with nitrogen. All blend films had to be processed from hot solutions in order to prevent premature aggregation of the polymers. Polymer/$PC_{71}BM$ solutions were spin-coated onto MoO_3 substrates, and then the films were left in Nitrogen atmosphere to dry. To deposit the electrodes, the samples were transferred into a vacuum chamber, and then LiF (0.6 nm)/ Al(100 nm) were deposited. The current density−voltage ($J-V$) characteristics of the OSCs were measured a source/measure unit (Keithley 4200) in the dark and under 100 mW cm^{-2} AM 1.5 G solar illumination in a N_2 -filled glove box. Light was generated with an Oriel 1-kW solar simulator referenced using a Reference Cell PVM 132 calibrated at the US National Renewable Energy Laboratory. A photomodulation spectroscopic set-up was used to measure the incident photon-to-current conversion efficiency as a function of light wavelength.

SCLC measurement. The electron-only devices with (ITO/Al/polymers:$PC_{71}BM$/Al) architecture and the hole-only devices with (ITO/MoO_3/PPhs:$PC_{71}BM$/MoO_3/Ag) architecture were fabricated. The electrical characteristics were measured using a source/measure unit (Keithley 4200) in a Nitrogen-filled glove box. J-V curves were fitted by using the Mott-Gurney square law. $J = (9/8)\, \varepsilon\mu\, (V^2/L^3)$, where ε is the static dielectric constant of the medium and μ is the carrier mobility.

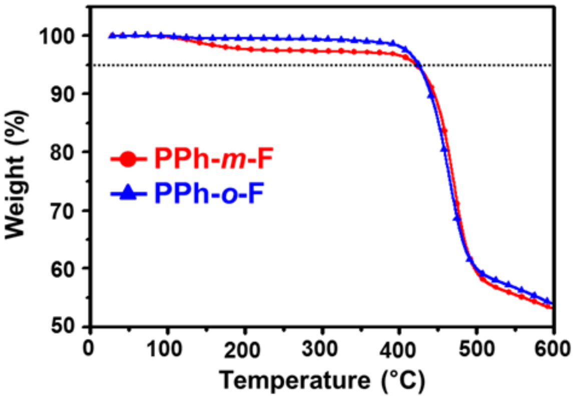

Figure S1. TGA plots of PPhs with a heating rate of 10 °C min^{-1}.

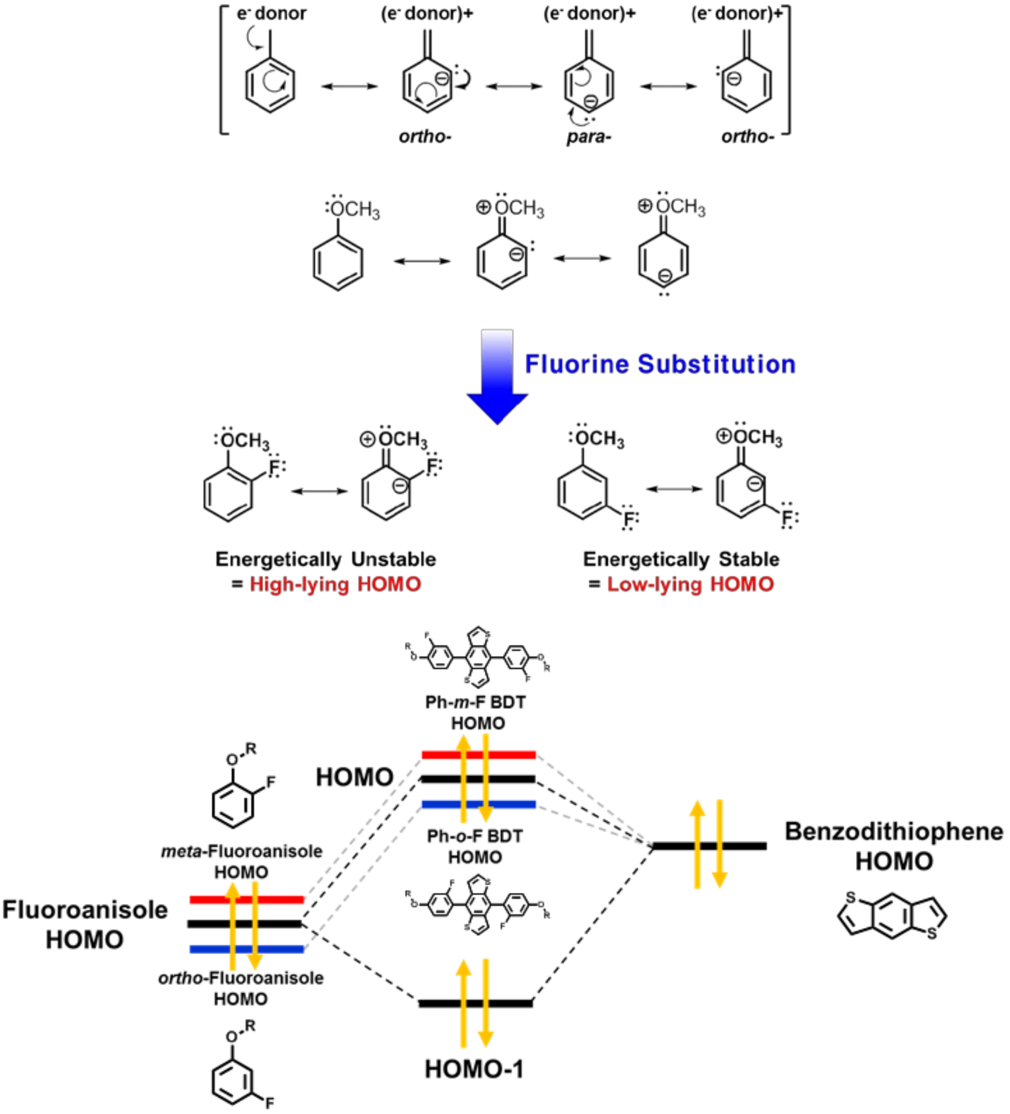

Figure S2. Resonance structures of side chains and molecular orbital hybridizations in the donor BDT with fluorinated phenyl side chains.

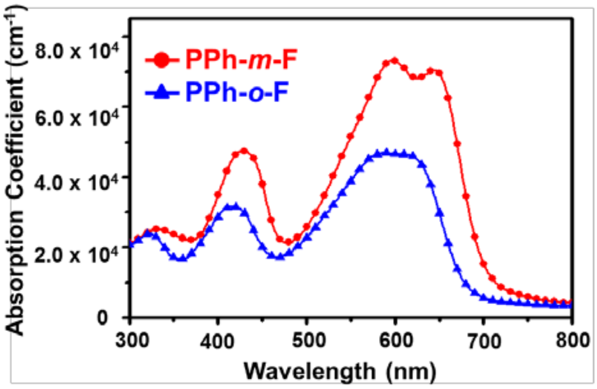

Figure S3. The calculated absorption coefficient of neat polymer film.

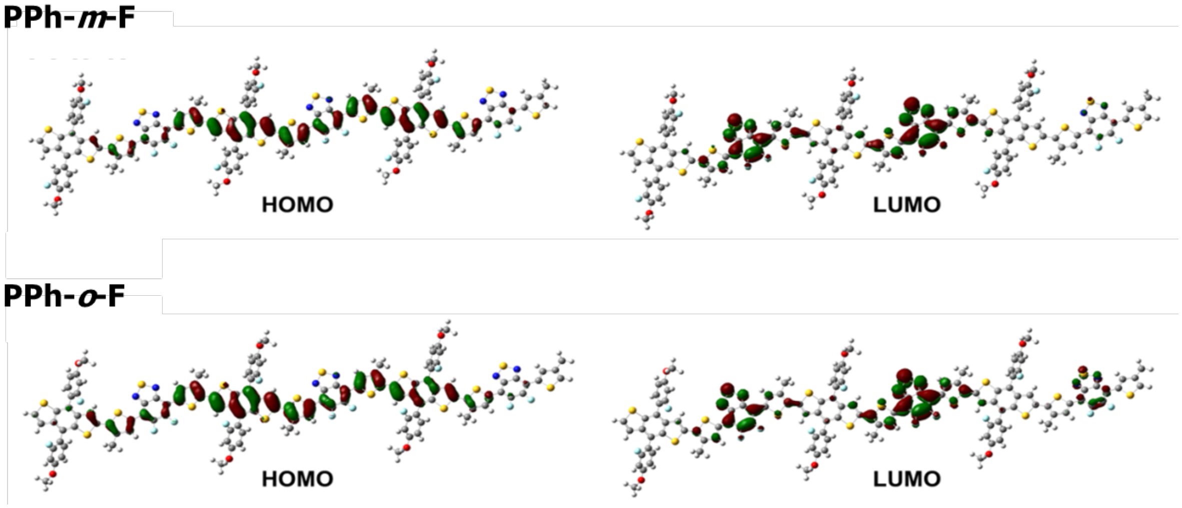

Figure S4. Calculated structure (B3LYP/6–31G) of the HOMO and LUMO of the model compounds. The yellow, red, blue and sky blue symbols represent sulfur, oxygen, nitrogen, and fluorine atoms, respectively.

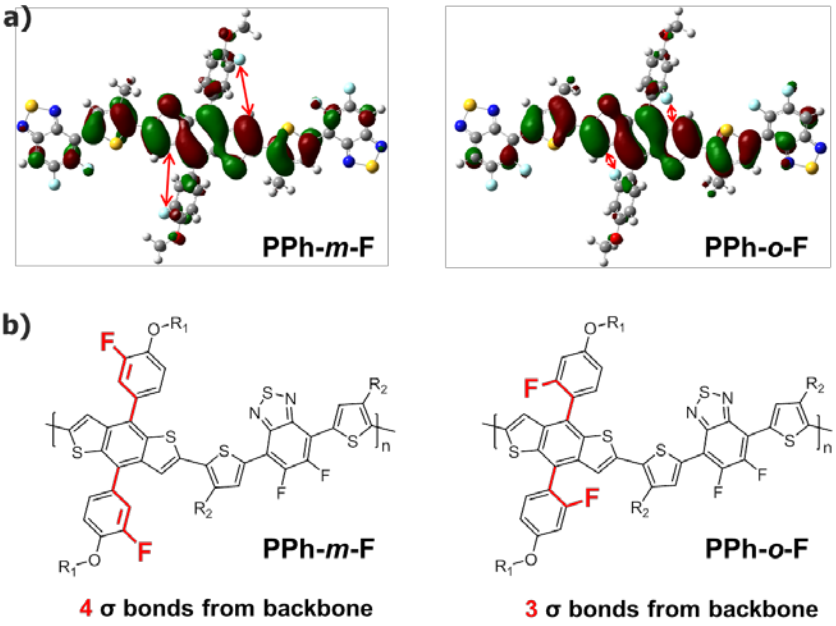

Figure S5. a) Distance of fluorine between HOMO along the backbone. b) Inductive effect is mainly affected from the length of σ bonds.

Table S1. Calculated dihedral angles of PPhs obtained from DFT calculations of energy-minimized structure (B3LYP/6-31G).

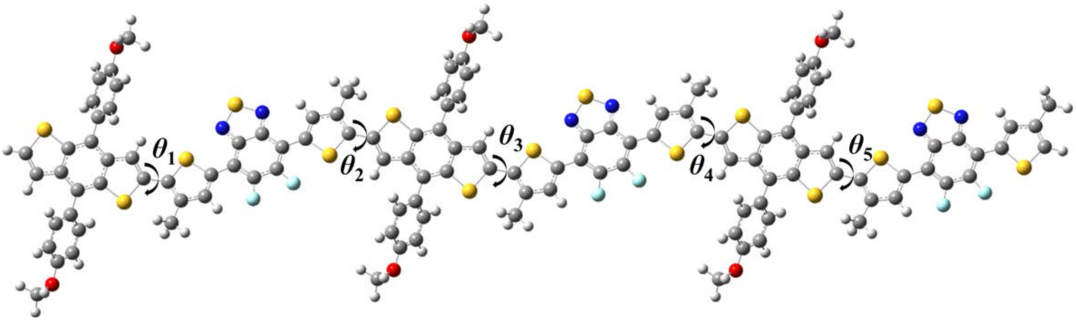

Polymer	$\theta_{1'}$ (deg)	θ_2 (deg)	θ_3 (deg)	θ_4 (deg)	θ_5 (deg)
PPh-*m*-F	21.5	23.8	16.7	21.7	18.5
PPh-*o*-F	25.2	23.7	22.2	22.3	24.9

Table S2. Standard deviation of the device performance. Blend weight ratios of PPhs:PC$_{71}$BM were fixed at 1:1.2 (w:w) with DIO 1.5 v% in DCB. Performance metrics are average numbers from eight devices of each type under the illumination condition of AM 1.5 G, 100 mW cm^{-2}. SCLC results measured by hole only device.

	Thickness [nm]	V_{oc} [V]	J_{sc} [mA cm^{-2}]	*FF* [%]	*PCE* [%]	Mobility [cm^2 V^{-1} s^{-1}]
PPh-*m*-F	119 ± 5.2	0.910 ± 0.009	11.15 ± 0.64	0.598 ± 0.028	6.07 ± 0.55	1.13×10^{-4} ± 0.15
PPh-*o*-F	105 ± 4.4	0.956 ± 0.012	4.66 ± 0.85	0.551 ± 0.058	2.43 ± 0.29	5.64×10^{-5} ± 0.23

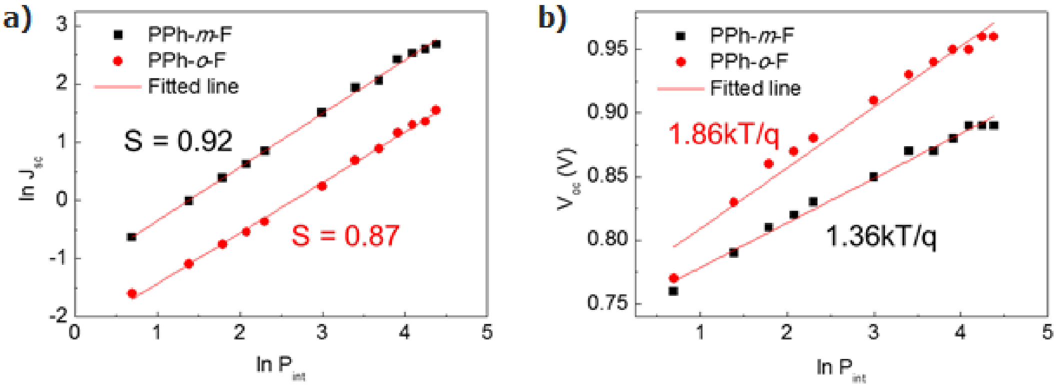

Figure S6. The measured (a) J_{sc} and (b) V_{oc} dependence on illumination intensity for PPh-*m*-F:PC$_{71}$BM blend and PPh-*o*-F:PC$_{71}$BM blend devices, together with linear fits to the data. V_{oc} is the maximum voltage a solar cell can provide to an external circuit, which is mainly derived from the molecular orbital energies of the heterojunction components. Meanwhile, the V_{oc} can also be influenced by various factors, e.g., charge recombination dynamics, film-processing conditions and choice of the device structure including the selection of electrodes.[3] Even though we fabricated identical device structures (ITO/MoO$_3$/active layer/LiF/Al) to prevent such subsidiary architectural effects on V_{oc}, charge recombination dynamics that originated from active layer material and morphology could influence the V_{oc} strongly.

The light-intensity dependent J_{sc} measurement was examined to investigate the nongeminate bimolecular recombination losses in the devices (Fig. S6a). The relationship between J_{sc} and incident light intensity, P_{int} can be described as $J_{\text{sc}} \propto P_{int}^{S}$. S should be equal to 1 if all dissociated free carriers are collected at the corresponding electrodes without charge recombination, while $S < 1$ indicates the presence of some extent of bimolecular recombination.[4,5] The PPh-*m*-F:PC$_{71}$BM and PPh-*o*-F:PC$_{71}$BM devices showed a big difference of J_{sc} dependencies on P_{light} with S of 0.92 for the

PPh-*m*-F:$PC_{71}BM$ device and 0.87 for the PPh-*o*-F:PCBM based device. These results indicate that the PPh-*m*-F:$PC_{71}BM$ device can sweep out charge carriers efficiently with weaker bimolecular recombination compared to that of the PPh-*o*-F:$PC_{71}BM$ device.

The recombination mechanisms can be further investigated according to the relationship of V_{oc} dependent on light intensity (Fig. S6b). The semilogarithmic plot of V_{oc} as a function of the light intensity shows a linear relationship with a slope of kT/q. If the Shockley−Read−Hall recombination, e.g. trap-assisted charge recombination, is involved, a stronger dependence of V_{oc} on the light intensity with a slope greater than kT/q will be observed.[6] The slope value of V_{oc}–$ln\ P_{int}$ curve of the PPh-*m*-F:$PC_{71}BM$-based solar cells was ~1.36kT/q. On the contrary, for the PPh-*o*-F:$PC_{71}BM$-based solar cells, the slope value was ~1.86kT/q, indicating that the V_{oc} loss is likely to be dominated by the combination of bimolecular and trap-assisted recombination.

These results show that non-geminate and trap-assisted recombination in the PPh-*o*-F:$PC_{71}BM$-based solar cells dominated more than those in the PPh-*m*-F:$PC_{71}BM$-based solar cells. This severe charge recombination in PPh-*o*-F:$PC_{71}BM$ device would increase the recombination current at the open circuit state of the photovoltaic device, hence reducing the maximum V_{oc} achievable from the molecular energy states of active layer materials.[7] These experimental results could explain the reason why the lowered HOMO energy level of the PPh-*o*-F polymer determined using CV did not show a linear increase of the V_{oc}.

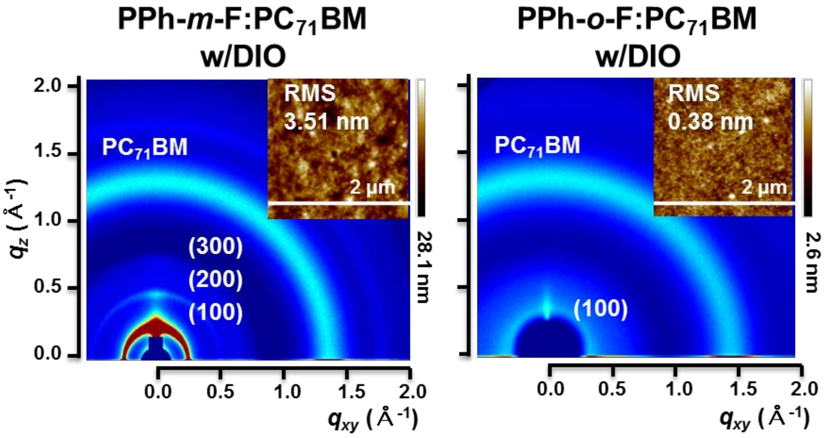

Figure S7. GIWAXS data of polymers/$PC_{71}BM$ (DIO) blend films. The insets are AFM height images (2.0 μm x 2.0 μm) of blend fims prepared by DCB with DIO for PPhs:$PC_{71}BM$. . The PPh-*m*-F blend film showed a rough surface because its low solubility and strong intermolecular interactions among polymers induced the aggregated domains during the formation of film. The high crystallinity and rough surface may have enhanced the internal light scattering and light absorption.

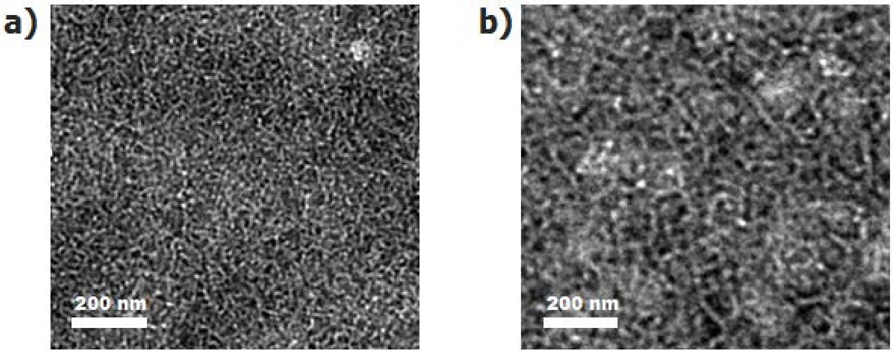

Figure S8. TEM images of blends a) PPh-*m*-F:$PC_{71}BM$, b) PPh-*o*-F:$PC_{71}BM$ with DIO. TEM images showed that relatively larger domain size within ~20 nm was observed in the TEM image of the PPh-*o*-F:$PC_{71}BM$ blend film (Fig. S8b) compared to the domain size with ~10 nm in the PPh-*m*-F:$PC_{71}BM$ blend film (Fig. S8a). This increased domain size can induce inefficient exciton dissociation at the polymer:$PC_{71}BM$ interface due to limited exciton diffusion length, hence reducing J_{sc}. Therefore, the PPh-*o*-F:$PC_{71}BM$ blend film had disadvantageous characteristics for photovoltaic performances, e.g. lower light absorption coefficient, lower charge carrier mobility, and larger domain size in bulkheterojunction morphology, compared to the PPh-*m*-F:$PC_{71}BM$ blend film.

References

(1) A. C. Stuart, J. R. Tumbleston, H. Zhou, W. Li, S. Liu, H. Ade and W. You, *J. Am. Chem. Soc*., 2013, **135**, 1806–1815.

(2) J. Shin, M. Kim, J. Lee, D. Sin, H. G. Kim, H. Hwang, K. Cho, *RSC Adv*., 2015, **5**, 106044-106052

(3) B. Qi, J. Wang, *J. Mater. Chem*., 2012, **22**, 24315

(4) P. Schilinsky, C. Waldauf, C. Brabec, *Appl. Phys. Lett*., 2002, **81**, 3885

(5) C. J. Brabec, M. Heeney, I. McCulloch, J. Nelson, *Chem. Soc. Rev.*, 2011, **40**, 1185.

(6) L. J. A. Koster, V. D. Mihailetchi, H. Xie, P. W. M. Blom, *Appl. Phys. Lett.*, 2005, **87**, 1.

(7) A. Maurano, R. Hamilton, C. G. Shuttle, A. M. Ballantyne, J. Nelson, B. O'Regan, W. Zhang, I. McCulloch, H. Azimi, M. Morana, C. J. Brabec, and J. R. Durrant, *Adv. Mater.*, 2010, **22**, 4987.